Microchim Acta (2010) 171:1–9
DOI 10.1007/s00604-010-0321-5

ORIGINAL PAPER

Characterization of graphite–polyurethane composite electrodes modified with organofunctionalized SBA-15 nanostructured silica in the presence of heavy metal ions. Application to anodic stripping voltammetry

Ivana Cesarino · Éder T. G. Cavalheiro · Christopher M. A. Brett

Received: 28 November 2009 / Accepted: 18 February 2010 / Published online: 28 March 2010

Abstract A graphite–polyurethane composite electrode with Santa Barbara Amorphous 15, SBA-15, mesoporous silica organofunctionalized with 2-benzothiazolethiol (BTSBA) as bulk modifier has been characterized electrochemically by voltammetry and electrochemical impedance spectroscopy (EIS) in the presence of cadmium ions, as an example of a toxic trace heavy metal, as well as by solid-state ^{13}C-NMR and by scanning electron microscopy. EIS measurements performed on the modified composite electrodes to investigate the influence of BTSBA on the deposition of cadmium during square wave anodic stripping voltammetry showed that organofunctionalization of the SBA-15 bulk modifier in the composite electrode facilitates heavy metal deposition. Experiments were also carried out with a mixture of submicromolar cadmium, lead, copper and mercury ions and led to similar conclusions.

Keywords Graphite–polyurethane composite electrode · SBA-15 nanostructured silica · 2-benzothiazolethiol · Electrochemical impedance spectroscopy · Trace heavy metals

I. Cesarino · É. T. G. Cavalheiro
Departamento de Química e Física Molecular,
Instituto de Química de São Carlos,
Av. Trabalhador São-Carlense, 400, Centro,
São Carlos, São Paulo CEP 13566-590, Brazil

C. M. A. Brett (✉)
Departamento de Química, Faculdade de Ciências e Tecnologia,
Universidade de Coimbra,
3004-535 Coimbra, Portugal
e-mail: brett@ci.uc.pt

Introduction

Increasing demands for ever more sensitive chemical sensors for environmental monitoring, air-quality detection, inflammable-gas inspection, healthcare, industrial production, and other applications have led to an upsurge of research devoted to the development of new sensing materials [1–5]. The new generation of sensing materials should exhibit a wide operation temperature range, high sensitivity, rapid speed, good accuracy, reproducibility, durability, easy processing and low cost. Recently, mesoporous materials, owing to their structural characteristics (ordered nanometer-size pore distributions, high pore volumes and high surface areas [6–9]) combined with the possibility to process them in various shapes (calibrated spherical powders, thin films, membranes, and monoliths [10–13]), have attracted much interest due to their potential applications in optoelectronics [14–16], catalysis [17–20], and sensors [21–26].

One of the more successful types of composite for electrochemical sensors is the carbon paste electrode prepared from an intimate mixture of graphite and an organic liquid. However, these electrodes have the serious disadvantage of limitations in their use in non-aqueous solvents [27]. Solid composite carbon electrodes, prepared with polymer matrices, do not suffer from this problem and are of interest for electrochemical analysis in such media, also showing a number of improved properties with respect to carbon paste such as surface regeneration by polishing, rigidity and ease of fabrication [28]. In this context, we previously proposed a rigid graphite-polyurethane composite electrode for use in electroanalysis [29].

Electrochemical impedance spectroscopy (EIS) is a powerful, non-destructive, informative, and amenable tech-

nique to examine an electrochemical system and electrode assembly, since the interfacial impedance of the electrode/solution is influenced by specific microscopic events of interest. EIS is becoming increasingly widely used in the field of electrochemical sensors and biosensors, mainly for characterization of the sensor assemblies, but also as a diagnostic and as a quantitative detection method [30]. Modelling of the interfacial region allows the determination, for a simple reaction, of electrode parameters such as the cell resistance (R_Ω) in series with a parallel combination of a constant phase element CPE (considered a non-ideal capacitance C with exponential factor α), and a charge transfer resistance (R_{ct}), attributed to the electrode/solution interface, from the impedance spectra [31, 32].

The purpose of this paper is characterization of graphite-polyurethane composite electrodes bulk-modified by Santa Barbara Amorphous 15 (SBA-15) mesoporous silica organofunctionalized with 2-benzothiazolethiol (BTSBA); SBA-15 has pores of size 4.6 to 30 nm [33]. This was done mainly by EIS, supported by solid-state NMR and scanning electron microscopy with the aim of observing the interaction of the modifier with trace cadmium ions, chosen as an example of toxic heavy metal ions, that can be quantified by square wave anodic stripping voltammetry. Changes at the electrode-solution interface occurring when analysing a mixture of cadmium, lead, copper and mercury ions were also evaluated.

Experimental

Instrumentation

Electrochemical measurements were carried out in a 20 mL total capacity thermostatted glass cell at 24 °C, using a graphite–polyurethane electrode modified with BTSBA as working electrode, saturated calomel electrode (SCE) and platinum wire as reference and auxiliary electrodes respectively. Voltammetric experiments were performed with a μAutolab Type III PGSTAT (Ecochemie, Netherlands) potentiostat/galvanostat coupled to a personal computer and controlled with GPES 4.9 software.

Electrochemical impedance spectra were recorded using a Solartron 1250 Frequency Response Analyser coupled to a Solartron 1286 Electrochemical Interface (Solartron Analytical, UK), controlled by ZPlot software, scanning the frequency logarithmically from 65.5 kHz to 0.1 Hz or 0.01 Hz, in 10 steps per frequency decade, with a sinusoidal perturbation of 10 mV rms amplitude superimposed on the chosen potential. Fitting to equivalent circuits was done with ZView software.

Solid state nuclear magnetic resonance (NMR) data for ^{13}C were obtained on a Varian INOVA spectrometer and scanning electron microscopy (SEM) images were recorded with a LEO-440 (Leica-Zeiss) microscope using a 20 kV electronic beam and magnification of 1000x.

Reagents and solutions

All chemicals were of analytical grade and were used without further purification. Solutions were prepared with water purified in a Millipore Milli-Q system (resistivity ≥ 18 MΩ cm). A 0.10 mol L^{-1} potassium chloride (Fluka, Switzerland) electrolyte solution was used for most experiments.

3-(chloropropyl)-trimethoxysilane (Aldrich, Germany) and 2-benzothiazolethiol (Sigma. Germany) were used in the organofunctionalization of the SBA-15 silica, carried out according to a previously-described procedure [34], as follows. A mass of 3.0 g of SBA-15 silica was refluxed with 2 ml of 3-(chloropropyl)-trimethoxysilane in 40 ml dry xylene for 24 h to introduce 3-chloropropyl on the surface. Following this, a sample of 3-chloropropyl SBA-15 silica was suspended in a N,N′-dimethylformamide solution containing 2-benzothiazolethiol with constant stirring and refluxing during 24 h. The functionalized particles were then treated with hot ethanol in a Soxhlet extractor during 8 h to eliminate excess organoalcoxysilane. Finally, the product was dried in air at 80 °C for 12 h. The BTSBA product is highly s and was stored at room temperature in a dry atmosphere until needed.

Graphite powder of 1–2 μm particle size (Aldrich, Germany) and polyurethane resin (Poliquil, Araraquara, SP, Brazil) were used for the preparation of the composite, see below.

A standard 1000 mg L^{-1} Cd^{2+} solution (Tec-Lab, Brazil, traceable to SRM 3108 NIST, USA); 1000 mg L^{-1} Pb^{2+} solution (Tec-Lab, Brazil, traceable to SRM 3128 NIST, USA); 1000 mg L^{-1} Cu^{2+} solution (Tec-Lab, Brazil, traceable to SRM 3114 NIST, USA) and 1000 mg L^{-1} Hg^{2+} solution (Tec-Lab, Brazil, traceable to SRM 3133 NIST, USA) were used for the preparation of the working cadmium, lead, copper and mercury solutions.

Preparation of the modified composite electrodes

The polyurethane (PU) resin was prepared by mixing 0.8 parts of pre-polymer (A-249) with 1.0 part of polyol (491-ID), according to the manufacturer's instructions, in the form of rods of 4 mm diameter and 50 mm length. Previous results [29] showed that the best composition of the material was 60% (*w/w*) graphite and 40% (*w/w*) PU. Modified composites were prepared by substituting corresponding amounts of the graphite powder and PU by BTSBA to obtain the desired composition. In one series of compositions, the proportion of PU was

fixed at 40% (*w/w*) and part of the graphite powder was replaced by the modifier in order to prepare electrode materials containing 5, 10, 15, 20% of BTSBA (*w/w*). In a second series, the proportion of graphite powder was fixed at 60% (*w/w*) and the PU was partially replaced by BTSBA—however, it was only possible to prepare this type of rod with 5 and 10% (*w/w*) of BTSBA, since when larger amounts of PU are substituted, homogenization becomes difficult.

The electrode was prepared from rods of the 4 mm diameter composite extruded in a press [29]. Rods of length 50 mm were cut and attached to a copper wire using silver epoxy (Electron Microscopy Sciences, Hatfield, PA, USA) and left to cure for 24 h. The electrode was sealed in a glass tube using epoxy resin (Silaex, São Paulo, SP, Brazil) and used only after at least 24 h curing, and the excess of polymer was removed using 600-grit abrasive paper. Finally, the electrode surface was polished with 1 μm γ-Al_2O_3 suspension on a polishing wheel and the electrode sonicated for 5 min, in water.

Results and disscussion

Characterization of the organofunctionalized SBA-15 silica and the composite electrode chemically modified with BTSBA

The organofunctionalization of the SBA-15 silica with 2-benzothiazolethiol was evaluated by solid-state NMR and SEM was employed for examining the surface modification of the composite electrode.

The ^{13}C-NMR spectra of the BTSBA (Fig. 1) show signals at 10.7, 23.7 and 36.6 ppm, that can be assigned to the methylene groups 1, 2 and 3, respectively. Carbon atoms of the heterocycle resonate at lower fields: 65.5 and 121.5 ppm (4 and 5, respectively). NMR data thus showed that the functionalization process occurs mainly by bonding of the thiol group with 3-(chloropropyl)-trimethoxysilane, previously fixed on the silica matrix, demonstrated through observation of CH_2-S bonds.

Scanning electron micrographs are presented in Fig. 2 and reveal changes in the surface morphology of the bulk-modified composite electrodes, both by SBA-15 silica alone and by BTSBA. It is thus possible to observe the influence of the incorporation of the modifiers in the graphite-PU composite electrode.

Influence of the electrode composition

The influence of the composition of the electrode material on the voltammetric response of the electrode bulk-modified with BTSBA was evaluated by square wave anodic stripping voltammetry (SWASV) of 4 μmol L^{-1} Cd^{2+} in 0.10 mol L^{-1} potassium chloride solution pH 3.0 and is presented in Fig. 3. Pre-concentration of Cd^{2+} was done for 120 s at −1.1 V, the square wave scan was done at a frequency of 50 Hz, 50 mV pulse amplitude and step potential of 5 mV. No response from oxidation of BTSBA was found in the potential range up to 0.5 V in blank experiments.

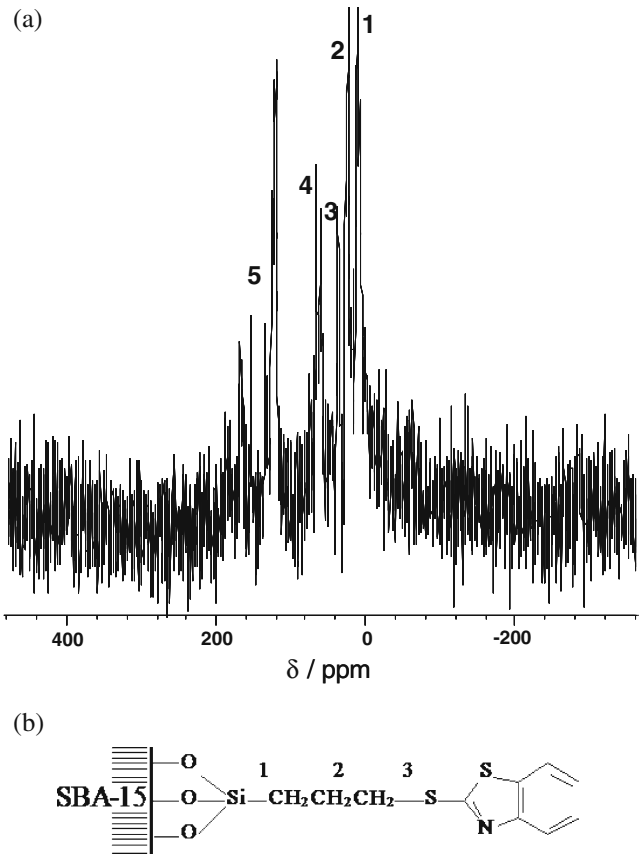

Fig. 1 **a** ^{13}C NMR spectrum of BTSBA in deuterated chloroform **b** structure of 2-benzothiazolethiol-modified SBA-15 (BTSBA), showing the three methylene groups in the ^{13}C NMR spectrum

The anodic peak current increased significantly when the amount of graphite powder was fixed at 60% (*w/w*) and substituting some of the PU by BTSBA, probably due to the higher content of the conducting phase at the electrode surface. The material of composition 5% (*w/w*) BTSBA, 60% (*w/w*) graphite and 35% (*w/w*) PU (Fig. 3e) was chosen for further studies because it presented higher anodic peak currents than that of composition 10% (*w/w*) BTSBA, 60% (*w/w*) graphite and 30% (*w/w*) PU (Fig. 3f).

Comparison of stripping voltammetric behaviour of Cd^{2+} at modified and unmodified composite electrodes

Figure 4 presents square wave anodic stripping voltammograms obtained with unmodified, SBA-15 silica modified and BTSBA-modified composite electrodes in 0.10 mol L^{-1}

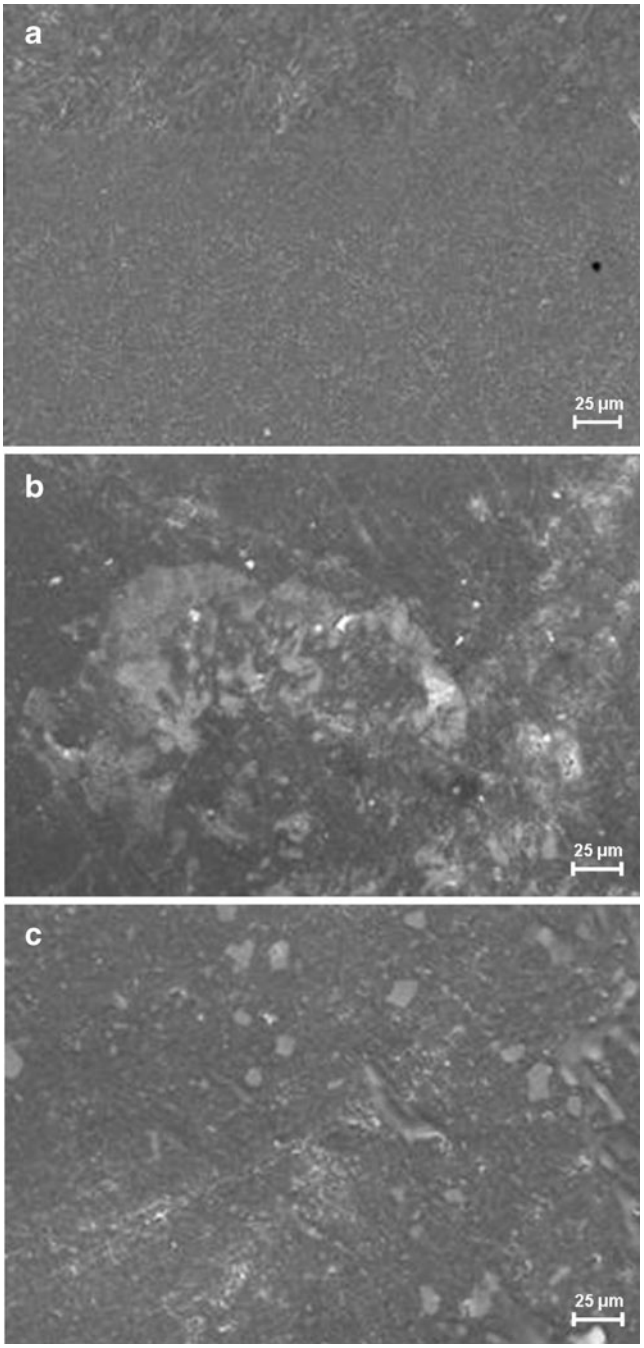

Fig. 2 Scanning electron micrographs of **a** unmodified electrode, **b** silica-modified composite electrode (5% SBA-15) and **c** BTSBA-modified composite electrode (5% of BTSBA)

potassium chloride solution pH 3.0. No peaks were observed in the potential range −1.1 to −0.6 V *vs.* SCE at the BTSBA bulk-modified composite electrode (curve a) in the absence of Cd^{2+}.

However, when the accumulation process was carried out for 120 s at −1.1 V in a solution containing 8 µmol L^{-1} Cd^{2+}, at the unmodified composite electrode (curve b), the Cd^{2+} oxidation peak appears at −0.77 V, the

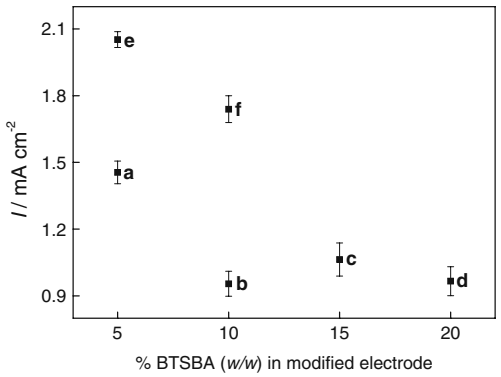

Fig. 3 Effect of the electrode composition containing different proportions of graphite, PU and BTSBA (*w*/*w*) respectively: **a** 55%, 40%, 5%; **b** 50%, 40%, 10%; **c** 45%, 40%, 15%; **d** 40%, 40%, 20%; **e** 60%, 35%, 5%; **f** 60%, 30%, 10%

SBA-15 silica modified composite electrode (curve c) exhibits an anodic peak at −0.74 V and the BTSBA-modified composite electrode (curve d) the Cd oxidation peak appears at −0.74 V, with a larger anodic current compared to that at the other electrodes. The increase in stripping currents at the modified composite electrode demonstrates that the organofunctionalization of SBA-15 nanostructured silica with 2-benzothiazolethiol plays an important role in the accumulation process of Cd^{2+} on the electrode surface, with advantages of increased sensitivity.

These questions have been explored in more detail in [35] and nanomolar detection limits have been achieved. The linear range remains the same as at the unmodified electrode, up to 1 µM, and the sensitivity increases by a factor of two.

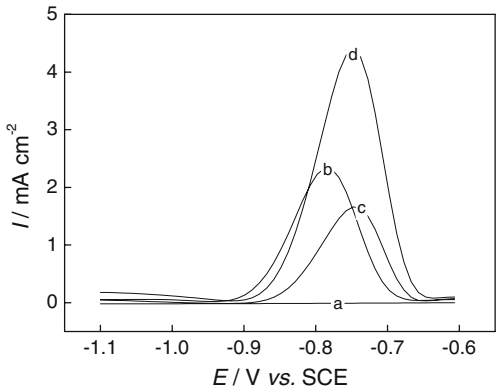

Fig. 4 Square wave anodic stripping voltammograms obtained in 0.10 mol L^{-1} KCl solution pH 3.0 for: **a** BTSBA-modified composite electrode, **b** unmodified composite electrode in the presence of 8 µmol L^{-1} Cd^{2+}, **c** SBA-15 silica-modified composite electrode in the presence of 8 µmol L^{-1} $Cd^{2+}$and **d** BTSBA-modified composite electrode in the presence of 8 µmol L^{-1} Cd^{2+}. Accumulation time 120 s; stripping parameters: potential interval −1.1 to −0.6 V *vs.* SCE, frequency 50 Hz, 50 mV pulse amplitude, step potential 5 mV

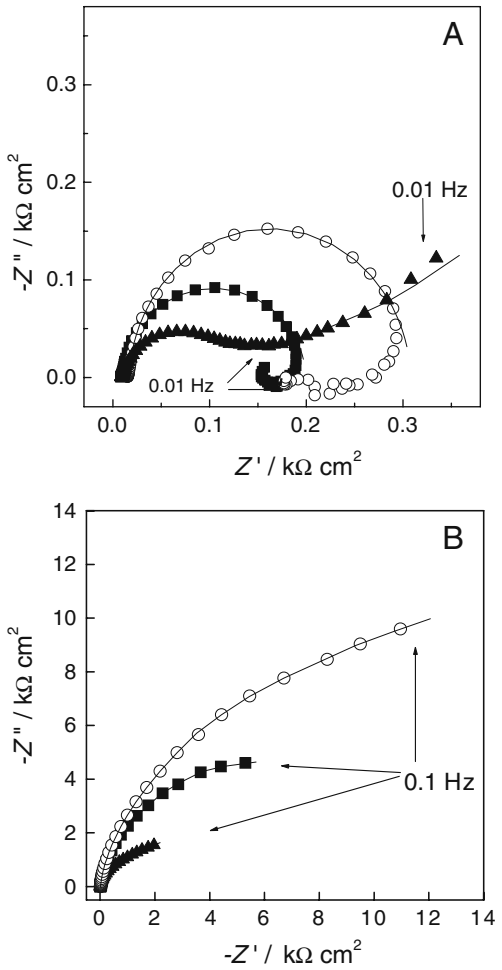

Fig. 5 Complex plane impedance plots **a** in the presence of Cd^{2+} / 0.10 mol L^{-1} KCl solution pH 3.0 and **b** only electrolyte for the composite electrodes: (▲) unmodified, (○) modified with SBA-15 silica and (■) modified with BTSBA. Lines show equivalent circuit fitting

Electrochemical impedance spectroscopy

Study of the electrochemical properties of modified graphite-PU composite electrodes

In order to understand better the influence of the bulk modification, EIS was used to investigate further the changes occurring in the interfacial region at unmodified and modified graphite-PU composite electrodes in the presence of Cd^{2+}. Experiments were carried out at the half-wave potential for cadmium oxidation, i.e. at −0.85 V for unmodified and at −0.84 V *vs* SCE for silica SBA-15 modified and BTSBA-modified composite electrodes. Figure 5 shows spectra in 0.1 M KCl solution pH 3.0 in the presence of cadmium ions (Fig.5a) and in their absence (Fig. 5b). In Fig 5a, all responses presented characteristic semicircles at high and medium frequencies, corresponding to charge transfer processes, and a diffusional process was observed at low frequencies at the unmodified electrode. For electrodes modified with silica SBA-15 and BTSBA, an inductive process is seen at low frequencies, probably due to adsorption of cadmium ions in the silica, causing blockage of the active sites of the electrode surface [36]. In the absence of Cd^{2+} (Fig. 5 b) these processes are not observed for any of the three types of composite electrode.

The high and middle frequency region of the spectra were fitted to an equivalent electrical circuit comprising the cell resistance, R_Ω, in series with a parallel combination of a constant phase element, CPE, and a charge transfer resistance, R_{ct}. The CPE is assumed to be a non-ideal capacitor of capacity C according to $CPE=\{(Ci\omega)^{\alpha}\}^{-1}$ where ω is the angular frequency and i the square root of −1, the roughness factor α varying from 0.5 to 1, where an α value of 1 represents a perfectly smooth and uniform surface. The fitting parameters obtained from Fig. 5a are shown in Table 1. It can be seen that the modified electrodes have a higher cell resistance and this fact can be explained by the adsorption of cadmium ions on the electrode surface, similarly to what was observed at carbon film electrodes [37]. Electrodes modified with SBA-15 mesoporous silica showed a higher value of the charge transfer resistance but a much lower charge separation (capacity) and a more uniform surface (higher α value). Functionalization with BTSBA reduces the charge transfer resistance, which is important for the occurrence of efficient charge transfer processes such as those in anodic stripping voltammetry, but charge separation is less affected.

Deposition of cadmium at the electrode modified with BTSBA

Experiments were carried out in the following sequence. Impedance spectra of the electrode modified with BTSBA were first recorded in 0.1 mol L^{-1} KCl solution pH 3.0 at −1.1 V and at −0.6 V *vs.* SCE. Following this, 0.5 μmol L^{-1} Cd^{2+} ions was added to the KCl solution and a potential of −1.1 V *vs.* SCE was applied to the working

Table 1 Summary of calculated EIS parameters obtained from Fig. 5a using the composite electrodes for cadmium ion oxidation in 0.10 mol L^{-1} KCl solution pH 3.0

Graphite-polyurethane electrode	R_Ω ($\Omega\cdot cm^2$)	R_{ct} ($k\Omega\cdot cm^2$)	C_1 ($\mu F cm^{-2}$ $s^{\alpha-1}$)	α
unmodified	9.5	0.12	349	0.83
modified with SBA-15 silica	16.0	0.31	43	0.98
+ BTSBA	11.0	0.18	82	0.98

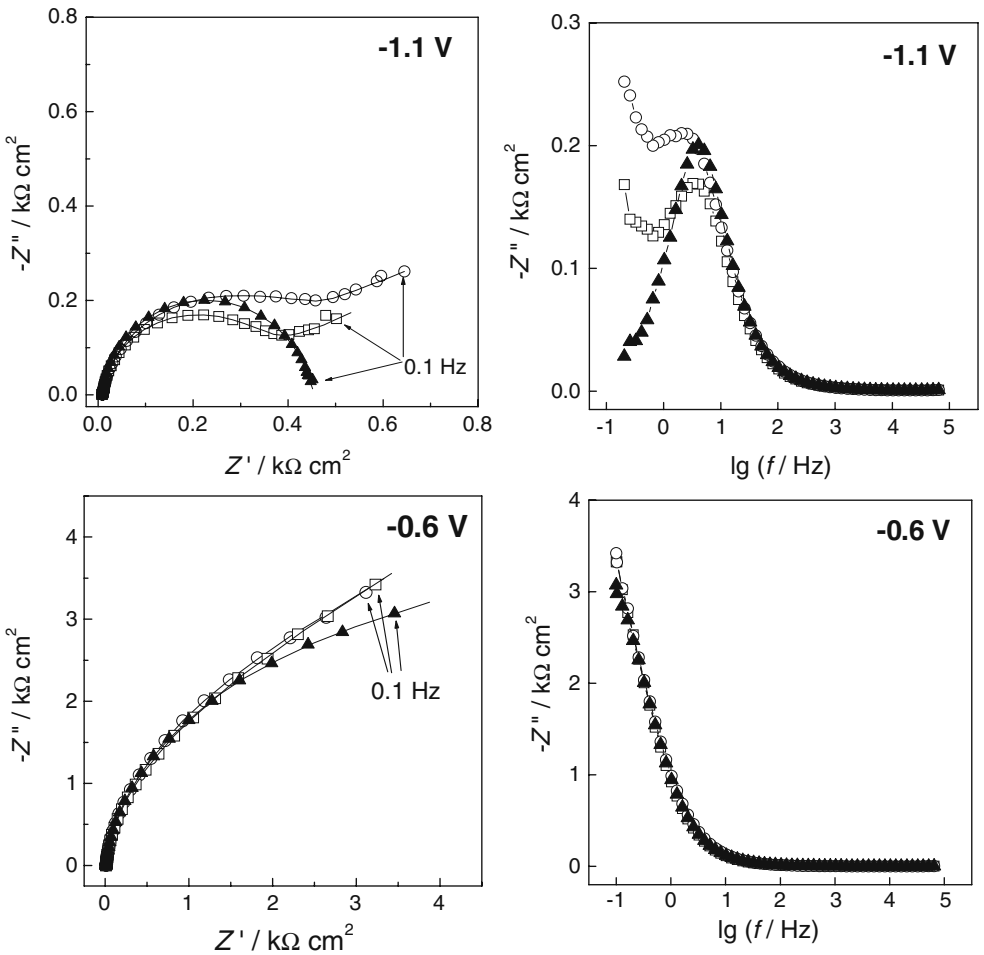

Fig. 6 Electrochemical impedance spectra as complex plane and $-Z''$ *vs.* lg (*f*/Hz) plots for composite electrode modified with BTSBA in 0.10 mol L^{-1} KCl solution pH 3.0 in the different situations: (□) electrolyte, (○) after Cd deposition and (▲) after SWASV. Lines show equivalent circuit fitting

electrode for 5 min in stirred solution, for metal deposition to occur. An impedance spectrum was then recorded at −1.1 V. After waiting 2 min with the electrode at open circuit for re-oxidation to occur, another spectrum was recorded at −0.6 V. Then, the electrode was placed in KCl solution and a "blank" SWASV experiment carried out to check the absence of metal ions. Finally, spectra were recorded at the same potentials of −1.1 V and −0.6 V, in order to ascertain if any permanent alteration to the surface of the modified electrode had occurred during the SWASV procedure.

The spectra obtained are shown in Fig. 6 as complex plane plots and as plots of the imaginary part of the impedance, $-Z''$, *vs.* lg (*f*/Hz), which aid in visualizing the differences in the adsorption behaviour and charge separation of the interfacial region. Semicircles in the complex plane plots, which are due to a resistance, *R*, and a capacitance, *C*, in parallel, lead to peaks in the $-Z''$ *vs.* lg (*f*/Hz) plots, and the maximum, when $\omega \cdot RC=1$ (ω in radians), corresponds to the time constant of the process.

Fitting of spectra was done using the same equivalent electrical circuit described above and the parameter values at −1.1 V are presented in Table 2. Values obtained under the different experimental conditions lie in the range 0.87–0.94 for α, the charge transfer and cell resistance increasing with the deposition of cadmium ions, which can be ascribed to complexation of Cd^{2+} with BT on the electrode surface. In the presence of Cd^{2+} ions, some alterations occur at low frequency, due to the adsorption of cadmium on the electrode surface. The peak in the $-Z''$ *vs.* lg *f* plot is at lg f=0.6 in electrolyte only, and with the addition of Cd^{2+}, shifts to a lower value (lg f=0.4), returning to its initial

Table 2 EIS parameters obtained at −1.1 V vs SCE for the BTSBA-modified graphite-PU composite electrode

Experiment	R_Ω (Ω cm^2)	R_{ct} (k$\Omega \cdot cm^2$)	C_1 (μF cm^{-2} $s^{\alpha-1}$)	α
Initially—electrolyte	8.71	0.42	170	0.88
+ Cd^{2+}	9.35	0.51	169	0.87
After SWASV	9.18	0.44	113	0.94

value after SWASV. There is a reduction in the interfacial capacity after SWASV and a more uniform surface, so permanent changes have occurred, see Table 2. Nevertheless, at −0.6 V, there are essentially no differences in the spectra obtained in the absence and presence of Cd^{2+}, where cadmium re-oxidation has occurred.

Simultaneous deposition of Cd^{2+}, Pb^{2+}, Cu^{2+} and Hg^{2+} at the graphite-PU electrode modified with BTSBA

EIS was also used to visualize the changes occurring when more than one metal is deposited. Experiments were carried out in the same sequence described previously, except that 10^{-7}mol L^{-1} Cd^{2+}, Pb^{2+}, Cu^{2+} e Hg^{2+} were simultaneously pre-concentrated at the modified electrode at −1.1 V and +0.15 V *vs.* SCE. An applied potential of −1.1 V is the optimized value for deposition of these metals [35] and +0.15 V corresponds to a potential more positive than that needed for re-oxidation of all the metals, the most positive being Hg^{2+} at +0.10 V.

Spectra obtained are shown in Fig. 7 in complex plane plots and as plots of the imaginary part of the impedance, $-Z''$, *vs.* lg (*f*/Hz). Using the same equivalent electrical circuit described above, the charge transfer resistance and the double layer capacitance at −1.1 V when only the electrolyte is present are respectively: 1.13 kΩ·cm^2 and 115 μF cm^{-2} s$^{\alpha-1}$. However, with the deposition of metal on the electrode surface these figures are: R_{ct}=0.78 kΩ·cm^2 and C_1 = 131 μF cm^{-2} s$^{\alpha-1}$ and after SWASV these values change to: R_{ct}=0.74 kΩ·cm^2 and C_1 = 215 μF cm^{-2} s$^{\alpha-1}$.

At −1.1 V, the peak in the $-Z''$ *vs.* lg (*f*/Hz) plot is at lg (*f*/Hz) = 1.8 for the modified electrode in the absence of the metals and with the accumulated metals shifts to higher values. The charge transfer resistance at the modified composite electrode is higher after the addition of Cd^{2+}, Pb^{2+}, Cu^{2+} and Hg^{2+} than with only cadmium ions, suggesting that deposition is easier when there is only Cd^{2+} in solution. At +0.15 V, after re-oxidation of the metals has occurred, there are no significant differences.

A further important point is that the charge transfer resistance (0.78 kΩ·cm^2) at the electrode modified with SBA-15 and BTSBA with addition of metal ions is significantly lower than those found in the literature (38.1 kΩ·cm^2 [37], and ~8.0 kΩ·cm^2 [38]).

These results suggest that the bulk-modified electrode described here is superior for the stripping voltammetry of heavy metals, due to better charge transfer kinetics for metal deposition.

Conclusions

Graphite–polyurethane composite electrodes modified with 2-benzothiazolethiol organofunctionalized SBA-15 silica

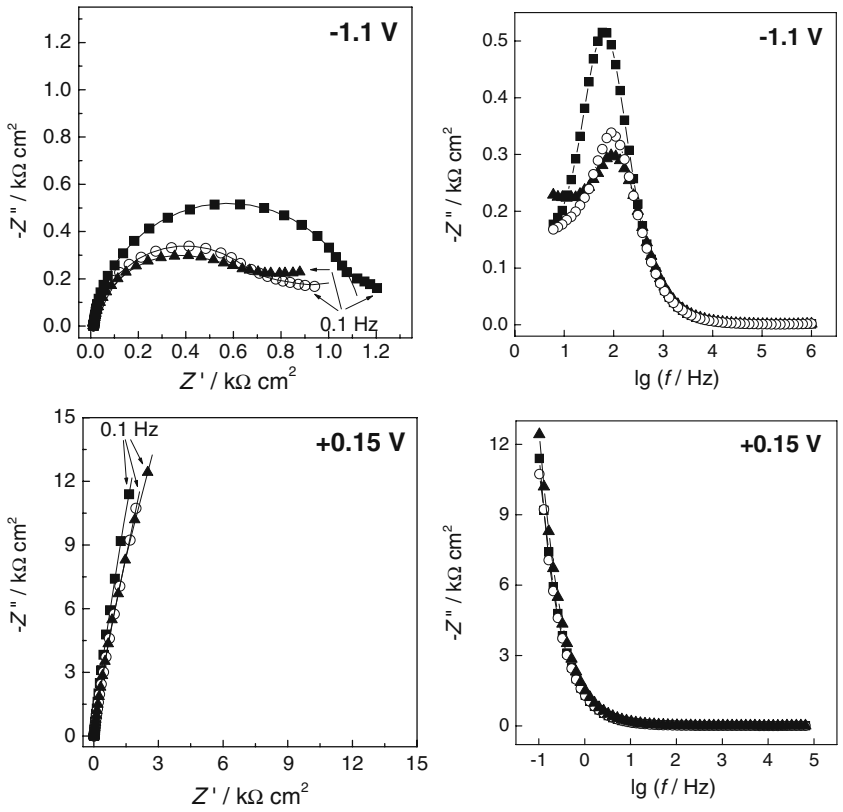

Fig. 7 Electrochemical impedance spectra as complex plane and $-Z''$ *vs.* lg (*f*/Hz) plots for composite electrode modified with BTSBA in the different situations: (▲) 0.10 mol L^{-1} KCl solution pH 3.0, (○) after Cd^{2+}, Pb^{2+}, Cu^{2+} and Hg^{2+} deposition and (■) after SWASV

have been characterized voltammetrically, by electrochemical impedance spectroscopy and by solid-state ^{13}C-NMR, with surface examination by SEM. The use of electrochemical impedance spectra has been exploited in order to follow the changes occurring at composite electrodes during square wave anodic stripping voltammetry of cadmium ions. Alterations due to metal ion deposition were observed and the potentiality of the modified composite electrode was investigated. The voltammetric and impedance results showed the advantages of BTSBA modification, which increases sensitivity in the accumulation process of Cd^{2+} and that the modified electrode facilitates heavy metal deposition, confirmed by carrying out experiments with a mixture of trace metal ions.

Acknowledgements Financial support from the Brazil/Portugal bilateral agreement (CAPES/FCT 177/07), FAPESP-Brazil (grant 08/03537-7), and from CEMUC® (Research Unit 285), FCT, Portugal is gratefully acknowledged.

References

1. Shimizu Y, Kai S, Takao Y, Hyodo T, Egashira M (2000) Correlation between methylmercaptan gas-sensing properties and its surface chemistry of SnO_2-based sensor materials. Sens Actuators B Chem 65:349–357
2. Ghica ME, Brett CMA (2008) Glucose oxidase inhibition in poly (neutral red) mediated enzyme biosensors for heavy metal determination. Microchim Acta 163:185–193
3. Zampolli S, Elmi I, Ahmed F, Passini M, Cardinali GC, Nicoletti S, Dori L (2004) An electronic nose based on solid state sensor arrays for low-cost indoor air quality monitoring applications. Sens Actuators B Chem 101:39–46
4. Im Y, Lee C, Vasquez RP, Bangar MA, Myung NV, Menke EJ, Penner RM, Yun M (2006) Investigation of a single Pd nanowire for use as a hydrogen sensor. Small 2:356–358
5. Sun YG, Wang HH (2007) High-performance, flexible hydrogen sensors that use carbon nanotubes decorated with palladium nanoparticles. Adv Mater 19:2818
6. Shibata H, Ogura T, Mukai T, Ohkubo T, Sakai H, Abe M (2005) Direct synthesis of mesoporous titania particles having a crystalline wall. J Am Chem Soc 127:16396–16397
7. Nandhakumar I, Elliott JM, Attard GS (2001) Electrodeposition of nanostructured mesoporous selenium films (H_I-eSe). Chem Mater 13:3840
8. Nishiyama N, Kaihara J, Nishiyama Y, Egashira Y, Ueyama K (2007) Vapor-phase synthesis of mesoporous SiO_2-P_2O_5 thin films. Langmuir 23:4746–4748
9. Yin J, Xiang L, Zhao X (2007) Monodisperse spherical mesoporous Eu-doped TiO_2 phosphor particles and the luminescence properties. Appl Phys Lett 90:113112
10. Brinker CJ, Lu Y, Sellinger A, Fan H (1999) Evaporation-induced self-assembly: Nanostructures made easy. Adv Mater 11:579
11. Baccile N, Grosso D, Sanchez C (2003) Aerosol generated mesoporous silica particles J. Mater Chem 13:3011–3016
12. Lu YF, Fan HY, Stump A, Ward TL, Rieker T, Brinker CJ (1999) Aerosol-assisted self-assembly of mesostructured spherical nanoparticles. Nature 398:223–226
13. Melosh NA, Lipic P, Bates FS, Wudl F, Stucky GD, Fredrickson GH, Chmelka BF (1999) Molecular and mesoscopic structures of transparent block copolymer-silica monoliths. Macromolecules 32:4332–4342
14. Gao F, Naik SP, Sasaki Y, Okubo T (2006) Preparation and optical property of nanosized ZnO electrochemically deposited in mesoporous silica films. Thin Solid Films 495:68–72
15. Anedda A, Carbonaro CM, Clemente F, Corpino R, Ricci PC (2005) Blue emission in mesoporous silica excited by synchrotron radiation. Opt Mater 27:958–961
16. Ozkan E, Lee SH, Liu P, Tracy CE, Tepehan FZ, Pitts JR, Deb SK (2002) Electrochromic and optical properties of mesoporous tungsten oxide films. Solid State Ionics 149:139–146
17. Suzuki TM, Yamamoto M, Fukumoto K, Akimoto Y, Yano K (2007) Investigation of pore-size effects on base catalysis using amino-functionalized monodispersed mesoporous silica spheres as a model catalyst. J Catal 251:249–257
18. Cortial G, Goettmann F, Mercier F, Floch PL, Sanchez C (2007) Bioinspired enantioselective catalysis: Racemic or achiral metal complexes grafted on mesoporous material functionalized with chiral molecules. Catal Commun 8:215–219
19. Jia M, Seifert A, Berger M, Giegengack H, Schulze S, Thiel WR (2004) Hybrid mesoporous materials with a uniform ligand distribution: Synthesis, characterization, and application in epoxidation catalysis. Chem Mater 16:877–882
20. Liu J, Yang Q, Kapoor MP, Setoyama N, Inagaki S, Yang J, Zhang L (2005) Structural relation properties of hydrothermally stable functionalized mesoporous organosilicas and catalysis. J Phys Chem B 109:12250–12256
21. Yang J, Hidajat K, Kawi S (2008) Synthesis of nano-SnO_2/SBA-15 composite as a highly sensitive semiconductor oxide gas sensor. Mater Lett 62:1441–1443
22. Keefe MH, Slone RV, Hupp JT, Czaplewski KF, Snurr RQ, Stern CL (2000) Mesoporous thin films of "molecular squares" as sensors for volatile organic compounds. Langmuir 16:3964–3970
23. Cesarino I, Cavalheiro ETG (2008) Thiol-functionalized silica thin film modified electrode in determination of mercury ions in natural water. Electroanalysis 20:2301–2309
24. Yamada T, Zhou HS, Uchida H, Honma I, Katsube T (2004) Experimental and theoretical NQ, physisorption analyses of mesoporous film (SBA-15 and SBA-16) constructed surface photo voltage (SPV) sensor. J Phys Chem B 108:13341–13346
25. Yuliarto B, Honma I, Katsumura Y, Zhou HS (2006) Preparation of room temperature NO_2 gas sensors based on W-and V-modified mesoporous MCM-41 thin films employing surface photovoltage technique. Sens Actuators B Chem 114:109–119
26. Cesarino I, Marino G, Matos JR, Cavalheiro ETG (2008) Evaluation of a carbon paste electrode modified with organofunctionalized SBA-15 nanostructured silica in the simultaneous determination of divalent lead, copper and mercury ions. Talanta 75:15–21
27. Klatt LN, Connell DR, Adams RE (1975) Voltammetric characterization of a graphite-teflon electrode. Anal Chem 47:2470–2472
28. Fernandez C, Reviejo AJ, Pingarron JM (1995) Development of graphite-poly(tetrafluoroethylene) composite electrodes-voltammetric determination of the herbicides thiram and disulfiram. Anal Chim Acta 305:192–199
29. Mendes RK, Claro-Neto S, Cavalheiro ETG (2002) Evaluation of a new rigid carbon-castor oil polyurethane composite as an electrode material. Talanta 57:909–917
30. Brett CMA (2008) Electrochemical impedance spectroscopy for characterization of electrochemical sensors and biosensors. ECS Trans 13:67–80

31. Brett CMA, Oliveira Brett AM (1993) Electrochemistry. Principles, Methods, and Applications. Oxford University Press, Oxford
32. Barsoukov E, Macdonald JR (2005) Impedance Spectroscopy, Theory, Experiment and Applications, 2nd edn. Wiley, New York
33. Zhao DY, Huo QS, Feng JL, Chmelka BF, Stucky GD (1998) Nonionic triblock and star diblock copolymer and oligomeric surfactant syntheses of highly ordered, hydrothermally stable, mesoporous silica structures. J Am Chem Soc 120:6024–6036
34. Cesarino I, Cavalheiro ETG, Marino G, Matos JR (2008) Functionalisation and characterization of SBA-15 nanostructured silica modified with 2-benzothiazolethiol. Mater Sci Forum 587–588:458–462
35. Cesarino I, Cavalheiro ETG, Brett CMA (2010) Simultaneous determination of cadmium, lead, copper and mercury ions using organofunctionalized SBA-15 nanostructured silica modified graphite-polyurethane composite electrode. Electroanalysis 22:61–68
36. Chen M, Du CY, Yin GP, Shi PF, Zhao TS (2009) Numerical analysis of the electrochemical impedance spectra of the cathode of direct methanol fuel cells. Int J Hydrogen Energy 34:1522–1530
37. Gouveia-Caridade C, Brett CMA (2006) The influence of Triton-X-100 surfactant on the electroanalysis of lead and cadmium at carbon film electrodes—An electrochemical impedance study. J Electroanal Chem 592:113–120
38. Gouveia-Caridade C, Pauliukaite R, Brett CMA (2006) Influence of Nafion coatings and surfactant on the stripping voltammetry of heavy metals at bismuth-film modified carbon film electrodes. Electroanalysis 18:854–861